VOL. 25, NO. 2, 2026, 70-77
elektrika.utm.my
EISSN 3083-9394

ELEKTRIKA
Journal of Electrical Engineering

3.5 GHz Microstrip Antenna Design with Specific Absorption Rate Analysis

Nurul Inshirah Mohd Razali[1], **Norhudah Seman**[1*] and **Nor Aishah Muhammad**[1,2]

[1]Wireless Communication Centre, Faculty of Electrical Engineering, Universiti Teknologi Malaysia, 81310 UTM Johor Bahru, Johor, Malaysia.
[2]Telecommunication Software and Systems, Faculty of Electrical Engineering, Universiti Teknologi Malaysia, 81310 UTM Johor Bahru, Johor, Malaysia.

[*]Corresponding author: huda@fke.utm.my

Abstract: This paper presents a fifth-generation (5G) 3.5 GHz microstrip antenna along with a specific absorption rate (SAR) analysis. The antenna is designed using basic microstrip antenna equations to determine its dimensions. The design employs a coaxial feeding method, with the optimal feeding location at P3 (10 mm, -6 mm) to achieve 50 Ω impedance matching. The antenna demonstrates good performance at 3.5 GHz, with a reflection coefficient, S_{11} of –27 dB and a gain of 2 dB. SAR is then assessed by placing the antenna at 10 mm from the head phantom. The presence of the head phantom affects antenna performance, resulting in a slight decrease in the resonant frequency due to head tissue conductivity. Furthermore, the presence of the head phantom modifies the radiation pattern and decreases radiated power as electromagnetic energy is dissipated within the phantom tissue. The SAR analysis indicates that the location of the coaxial feeding influences the SAR value, with the best location (P3) yielding the lowest SAR of 5.6 W/kg for 1 g and 2.33 W/kg for 10 g of tissue, with input power fixed at 0.25 W (23.98 dBm). The maximum permissible power for the proposed microstrip antenna is 0.07 W (18.45 dBm), resulting in SARs of 1.56 W/kg for 1g and 0.65 W/kg for 10g of tissue, respectively. Both values are within the standard SAR limit and are deemed safe for use.

Keywords: Antenna, Coaxial Feeding, Head Phantom, Microstrip, Specific Absorption Rate

Article History: received 16 July 2025; accepted 24 July 2026; published 31 August 2026
Digital Object Identifier 10.11113/elektrika.v25n2.769

1. INTRODUCTION

Wireless communication is essential for exchanging information among machines, vehicles, and various networked technologies, as well as between individuals worldwide. As the demand for faster, more reliable, and higher-capacity connectivity develops, fifth-generation (5G) wireless technology has emerged as a key solution. It substantially enhances network capacity, latency, and data rates by operating in sub-6 GHz and millimeter-wave bands [1]. The 3.5 GHz band is of particular significance in the sub-6 GHz band, which is categorized in Frequency Range 1 (FR 1), as it is extensively used for commercial 5G deployment due to its optimal balance of performance and coverage [2]. Antennas operating within sub-6 GHz frequencies, specifically at 3.5 GHz, necessitate a compact and efficient design and performance, as they can expand beyond fourth-generation (4G) capabilities to meet these demands [3]. One of the most widely used antennas in various applications is the microstrip antenna [4].

Microstrip antennas are widely used in modern wireless systems due to their low-profile structure, ease of fabrication, and integration with electronic circuits [5]. These characteristics make them particularly suitable for mobile communication applications [6]. However, mobile communication devices are typically operated near the human body, raising concerns about specific absorption rate (SAR) compliance and user safety. The placement of the antenna near biological tissue may lead to increased absorption of radio-frequency energy [7]. The International Commission on Non-Ionising Radiation Protection (ICNIRP) and the Federal Communications Commission (FCC) have established guidelines for the general public's exposure. These guidelines prescribe exposure limits, SAR of 2.0 W/kg averaged over a volume of 10 g of tissue [8] and 1.6 W/kg averaged over 1 g of tissue [9], specific to frequencies below 6 GHz.

Since the microstrip antenna is widely used in current and future generations of wireless communication systems, it is essential to study the SAR performance of the basic conventional microstrip design, which serves as the foundational structure prior to any modifications, to ensure compliance and comparison with future improved designs. Furthermore, the study in [10] reported that microstrip antennas tend to produce lower SAR values than PIFA and monopole antennas. Similarly, the works in [11] and [12] found that microstrip antennas have lower SAR than dipole antennas, and all microstrip antennas reported in [10], [11], [12] focus on using a line-feeding method.

Many researchers have presented microstrip antenna designs with SAR studies, such as a design featuring a U-shaped patch and a semi-circular slot in the ground with a line-fed configuration, as reported in [13]. The antenna, with an overall size of 42 x 42 mm, has SARs of 0.095 W/kg and 0.036 W/kg for the respective 1 g and 10 g of tissue at 3.3 GHz when the input power was fixed at 15 dBm (0.03 W). This article reported a modification of the antenna structure to achieve optimal S_{11} and gain, with a low SAR. However, the SAR was studied for the modified antenna structure, with no baseline comparison to the basic conventional design prior to the modification. A similar approach was presented in [7], where a hexagonal-shaped antenna with a slot in the middle, a defected ground structure, and a line-feeding configuration, resulting in good antenna performance, and low SAR. The antenna fed with an input power of 0.001 W exhibited SARs of 0.013 W/kg and 0.008 W/kg for 1 g and 10 g of tissue, respectively.

Meanwhile, a 28 GHz Frequency Range 2 (FR2) conventional basic-structure microstrip antenna with a line-feeding has been presented in [14]. By optimizing the size of the patch and ground, the antenna demonstrated well performance with -21 dB S_{11}, 7.3 dB gain, and the SARs of 1.68 W/kg and 0.121 W/kg for the respective 1 g and 10 g of tissue by using a 15 dBm input power. This article found that ground size can influence SAR, with a larger size improving gain and producing lower SAR. However, this article focused on FR2 with a line-feeding, which supposed to be assessed using absorbed power density (APD) instead [15]. Another microstrip antenna without modification has been designed at 3.5 GHz with an overall size of 80 mm width x 80 mm length [16], which can be considered quite large for a sub-6 GHz antenna with a line-fed configuration. The antenna exhibited good performance, with -50 dB S_{11} and 7 dB gain. However, the work in [16] did not investigate the SAR characteristics, which similar to [17], [18].

Thus, while numerous studies in [7], [10], [11], [12], [13], [14], have explored SAR of modified microstrip antennas with line-fed configuration, there is a notable lack of baseline SAR data for unmodified, conventional microstrip antennas using alternative feeding methods like coaxial probe. Although coaxial feeding generally offers superior performance and lower spurious radiation compared to line-feeding [19], [20], research on the SAR behavior of basic coaxially fed antennas remains limited. Without this foundational baseline data, it is difficult to determine whether changes in SAR are actually caused by structural modifications to the antenna. Furthermore, even studies that do examine conventional antenna structures typically rely on line-feeding and often omit SAR assessments altogether [16], [17], [18]. To address this gap in the literature, this paper establishes baseline SAR characteristics and identifies the maximum permissible input power to ensure the safe operation of a conventional coaxially fed microstrip antenna at 3.5 GHz.

Consequently, this paper is organized as follows: Section 2 discusses the antenna design and feeding method analysis. Section 3 presents the simulation findings, followed by the conclusion in Section 4.

2. ANTENNA DESIGN AND FEEDING METHOD ANALYSIS

The antenna is designed based on the basic theory and equations of a conventional microstrip antenna, as discussed in the following subsection, along with the analysis of the coaxial feeding method. This antenna is designed and analyzed using CST Microwave Studio software.

2.1 Microstrip Antenna Design Structure

A microstrip antenna utilizing coaxial feeding, is designed with Rogers RT5880 substrate, which features a dielectric constant of 2.2, a conductor coating of 0.035 mm, a substrate thickness of 0.252 mm, and a tangent loss of 0.009. The Rogers RT5880 substrate is chosen in this design because it offers a favorable combination of low loss tangent, low dielectric constant, and high Q-factor, making it the best substrate to be used [21]. The proposed conventional microstrip antenna consists of the patch, substrate, ground plane, and the feeding, as presented in Figure 1. Its perspective view is shown in Figure 2 with an extended height view of the patch, substrate, and ground plane layers. The microstrip antenna with a rectangular radiating element is designed utilizing equations (1) – (4) [22]:

$$W = \frac{c}{2f_r}\sqrt{\frac{2}{\varepsilon_{reff}+1}} \tag{1}$$

$$\varepsilon_{reff} = \frac{\varepsilon_r+1}{2} + \frac{\varepsilon_r-1}{2}\left(\frac{1}{\sqrt{1+\frac{12W}{h}}}\right) \tag{2}$$

$$L = \frac{c}{2f_r\sqrt{\varepsilon_{reff}}} - 2\Delta L \tag{3}$$

$$\frac{\Delta L}{h} = 0.412\frac{(\varepsilon_{reff}+0.3)\left(\frac{W}{h}+0.264\right)}{(\varepsilon_{reff}-0.258)\left(\frac{W}{h}+0.8\right)} \tag{4}$$

where W, c, f_r, ε_r, ε_{reff}, h, L, and ΔL denote the width of the patch antenna, speed of light, resonant frequency, dielectric constant, effective dielectric constant, substrate thickness, patch length, and extended incremental length of the patch, respectively. From the calculation, the width, W and length, L of the patch are obtained as 33.8 mm and 28.7 mm, respectively, as shown in Figure 3.

The coaxial feeding method is chosen for its well-known advantage of being easy for impedance matching through the adjustable feed position [23]. The proposed microstrip antenna's dimensions are presented in Figure 3,

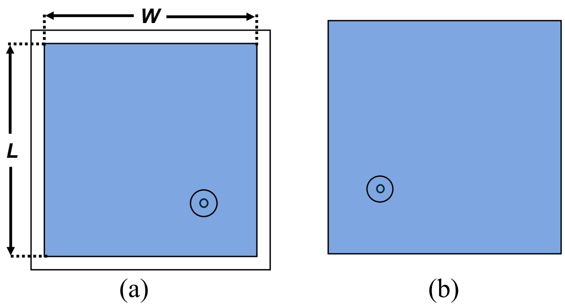

Figure 1. The proposed microstrip antenna at: (a) top view and (b) bottom view.

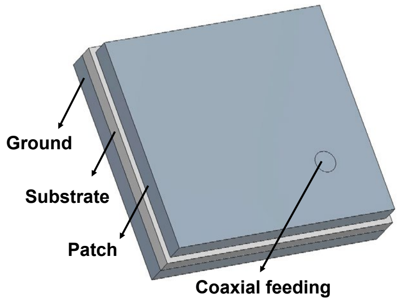

Figure 2. Perspective view of the proposed microstrip antenna.

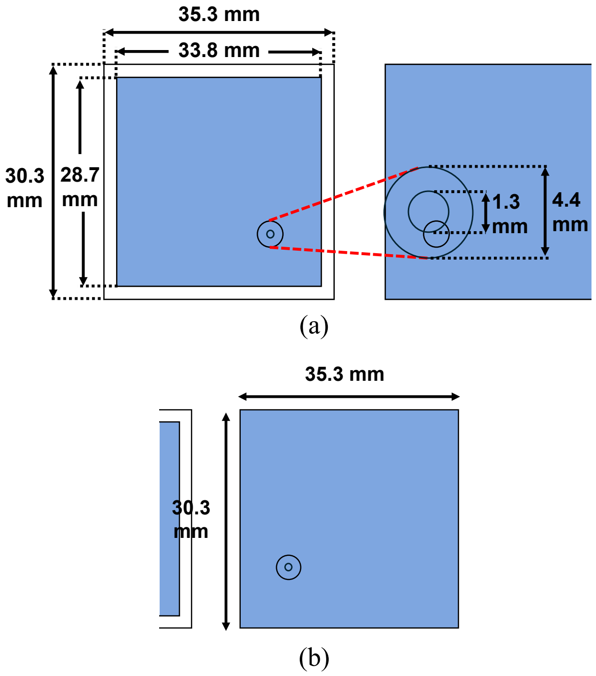

Figure 3. Dimensions of the proposed microstrip antenna at: (a) top view and (b) bottom view.

where all the dimensions are obtained upon calculation from the equations (1)-(4) without any size alteration. The coaxial feeding location is tuned and analyzed to match the impedance by finding its optimal position. This will be discussed further in the following subsection.

2.2 Feeding Method Analysis in Antenna Design

The feeding method used in this study is coaxial feeding. As illustrated in Figure 3(a), it consists of three layers, i.e., the inner layer is the pin that connects to the patch, the second layer is the dielectric of the feeding, which is Teflon, to isolate the pin and the outer conductor layer, and the outermost layer is the cover, which is connected to the ground plane [24]. The position of the feed is crucial for achieving 50 Ω impedance matching between the feed and the antenna, ensuring the antenna operates effectively. The position of the coaxial feeding is tuned to achieve optimal impedance matching. The position of the feed is placed and tested at four points, starting from P1 (10 mm, 6 mm), which is located at the top-right of the patch, to the middle-right side, P2 (10 mm, 0 mm) and the bottom-right of P3 (10 mm, -6 mm), then finally P4 (5 mm, -6 mm), as illustrated in Figure 4.

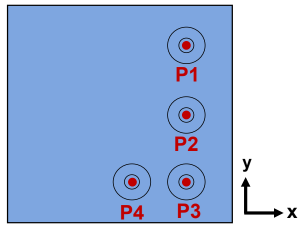

Figure 4. Four points are used to determine the feed location with the optimal 50 Ω matching.

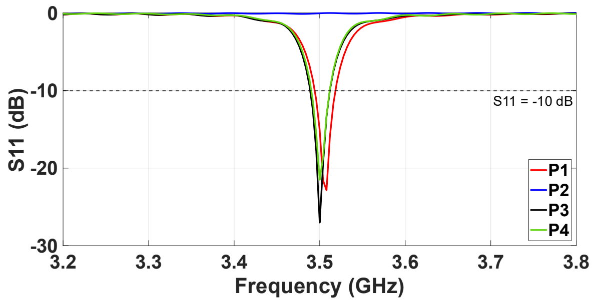

Figure 5. Antenna's S11 performance with four coaxial feeding locations.

Figure 5 shows that the best antenna matching occurs at P3 (10 mm, -6 mm), which has the best S_{11} of -27 dB. Meanwhile, the feeding locations of P1, P2, and P4 demonstrate S_{11} of -15 dB, -0.02 dB, and -21 dB, respectively.

Moreover, antenna gain and efficiency performance with four different feeding locations are obtained, indicating that the antenna with feeding at the P3 location has the highest gain of 2 dB and efficiency of 35%. The efficiency of the conventional microstrip antenna without modification is typically around ~30% [25]. Coaxially fed antennas typically achieve a lower gain of approximately 2 dB, which is considered satisfactory, compared to line-fed antenna designs (~6 dB) [26]. While for the efficiency, it can be enhanced by a few techniques, such as the implementation of the slot on the patch and ground plane to regulate current distribution effectively, and enhance the efficiency and overall radiation performance, including gain [27]. Meanwhile, the worst performance occurred at the feeding location of P2, with only -0.02 dB of S_{11}, indicating the antenna has very poor matching. The S_{11}, gain, and efficiency performance for different feeding locations are summarized in Table 1.

Table 1. Antenna performance for different coaxial feeding locations

Feeding location (x mm, y mm)	**S_{11} (dB)**	**Gain (dB)**	**Efficiency (%)**
P1 (10, 6)	-15	1.9	34
P2 (10, 0)	-0.02	-18	0.27
P3 (10, -6)	-27	2	35
P4 (5, -6)	-21	1.9	34

Therefore, the feeding location for the proposed microstrip antenna design is set to P3 (10 mm, -6 mm). The antenna will then be analyzed, and all the results will be discussed in the following section.

3. RESULTS AND DISCUSSION

The proposed microstrip antenna is analyzed under two conditions, i.e., without and with a head phantom. The analysis is conducted using CST Microwave Studio, from which the head model is also obtained. The antenna is located 10 mm from the head phantom, which is used to investigate the SAR performance, as shown in Figure 6. Meanwhile, the power is fixed to 0.25 W (23.98 dBm), which is within the range of the peak input power of the mobile phone [28]. A crucial element of antenna performance is the reflection coefficient, S_{11}. An effective antenna design generally demonstrates an S_{11} below –10 dB, signifying that less than 10% of the input power is reflected, while over 90% is effectively transmitted [29]. Figure 7 illustrates the S_{11} of the proposed conventional antenna, without and with a head phantom, achieving –27 dB and -13 dB, respectively, indicating excellent impedance matching. It demonstrates that the frequency shifts slightly when the antenna is placed near the head phantom, which might be due to the influence of the human tissue conductivity [30], and radiated power absorption.

Figure 8 illustrates the radiation pattern of the microstrip antenna of the E-plane and H-plane for antennas without a head phantom and antennas with a head phantom. It can be noticed that the head phantom alters the pattern of the antenna radiation, causing the radiated power to decrease at the main lobe due to the absorption and scattering by the head phantom [31]. In addition, the human body might distort the radiation pattern by forming sidelobes due to scattering by the head phantom, thereby compromising the antenna's performance [32]. The maximum gain of the antenna without the head phantom is 2 dB, which is considered a stable and acceptable gain [33].

Subsequently, the SAR performance of the proposed microstrip antenna is evaluated for different coaxial feed locations, namely P1, P2, P3 (the selected location), and P4, to investigate the influence of feed position on SAR characteristics. Figure 9 shows that the SAR results differ depending on the feeding locations. The lowest SAR is obtained at the P2 feeding location, with 0.03 W/kg and 0.01 W/kg for 1 g and 10 g of tissue, respectively, as illustrated in Figure 9 (c) and Figure 9 (d). This indicates that the microstrip antenna with feeding location at P2 exhibits poor impedance matching (S_{11} = -0.02 dB), resulting in ineffective radiation and poor power transmission, which explains a very low SAR. Meanwhile, the antenna with the best feeding location, P3, has lower SAR compared to P1 and P4 locations, with SARs of 5.6 W/kg and 2.33 W/kg for the respective 1g and 10 g of tissue. The SAR values for antennas with all feed locations are tabulated in Table 2.

Furthermore, the obtained SARs can be expressed by [34]:

$$SAR = \frac{\sigma\,|E|^2}{\rho}, \quad (5)$$

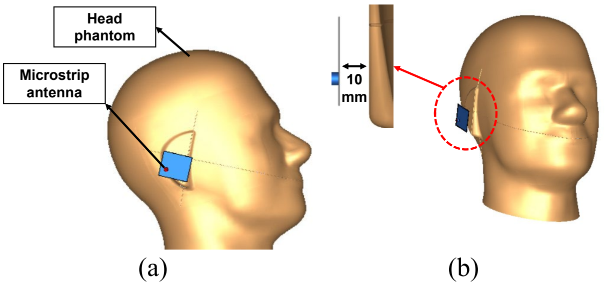

Figure 6. The proposed microstrip antenna with head phantom at: (a) side view, and (b) 10 mm gap between antenna and head phantom.

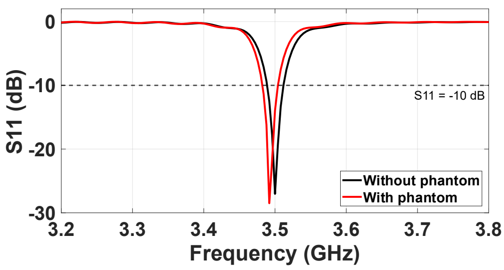

Figure 7. Reflection coefficient, S11 simulation results of the proposed microstrip antenna with and without phantom.

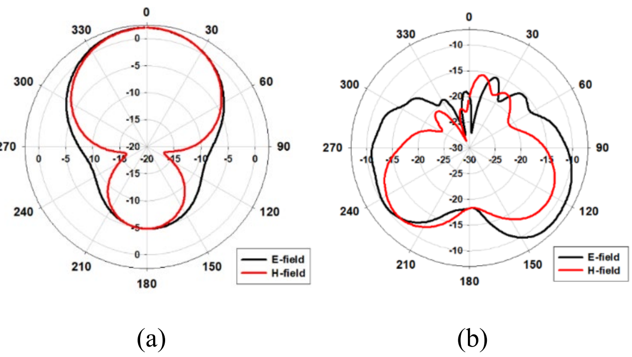

Figure 8. Radiation pattern of the proposed microstrip antenna: (a) without phantom and (b) with phantom

where $|E|$ denotes the magnitude of the RMS electric field strength, σ represents the tissue's conductivity, and ρ signifies the mass density of the tissue. It shows that SAR is proportional to the tissue's conductivity, σ, and the electric field strength, E, while being inversely proportional to the tissue's mass density, ρ. Thus, the following SAR simulation results are obtained as a function of the electric field strength inside the head phantom, which varies with different feeding locations.

Table 2. SAR performance of the designed microstrip antenna with the different feeding locations

Location of feeding (x mm, y mm)	SAR (W/kg)	
	1 g of tissue	10 g of tissue
P1 (10, 6)	5.85	2.49
P2 (10, 0)	0.03	0.01
P3 (10, -6)	5.6	2.33
P4 (5, -6)	6.84	2.71

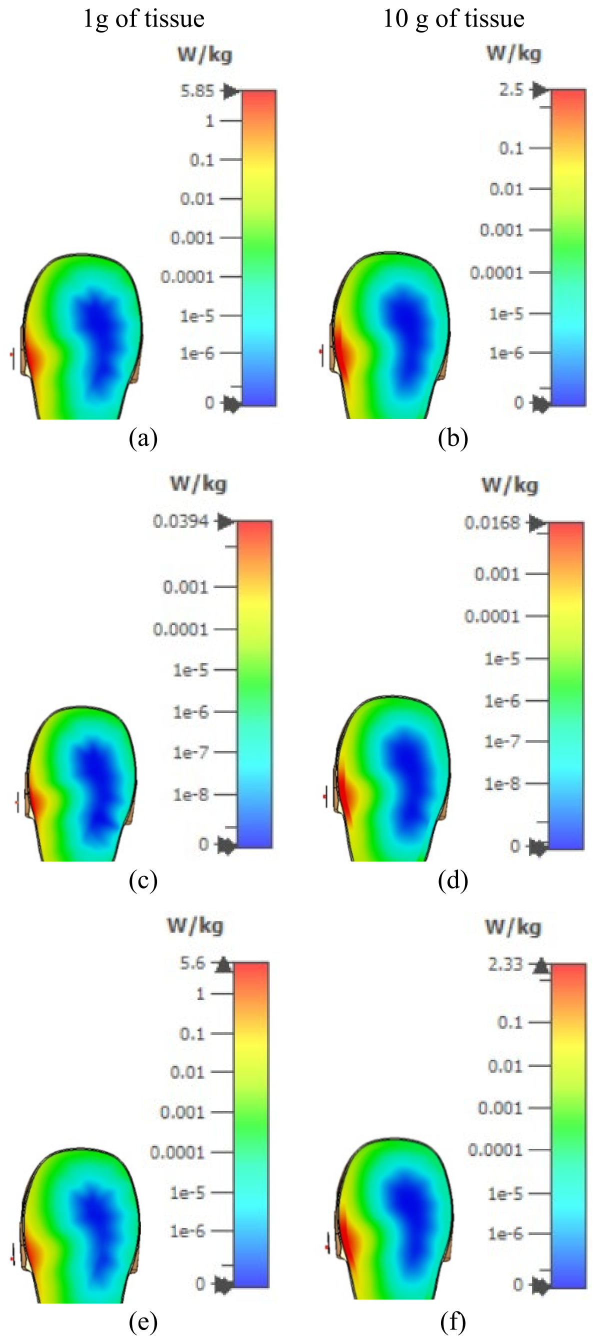

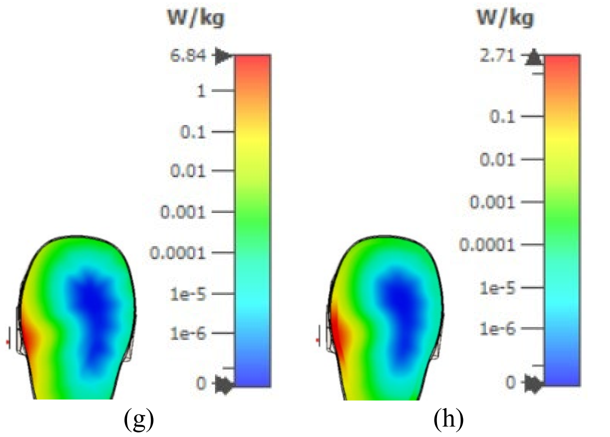

Figure 9. Visualization of SARs in the head phantom for feedings located at: (a) P1, (b) P1, (c) P2, (d) P2, (e) P3, (f) P3, (g) P4, and (h) P4 for the respective 1 g and 10 g of tissue.

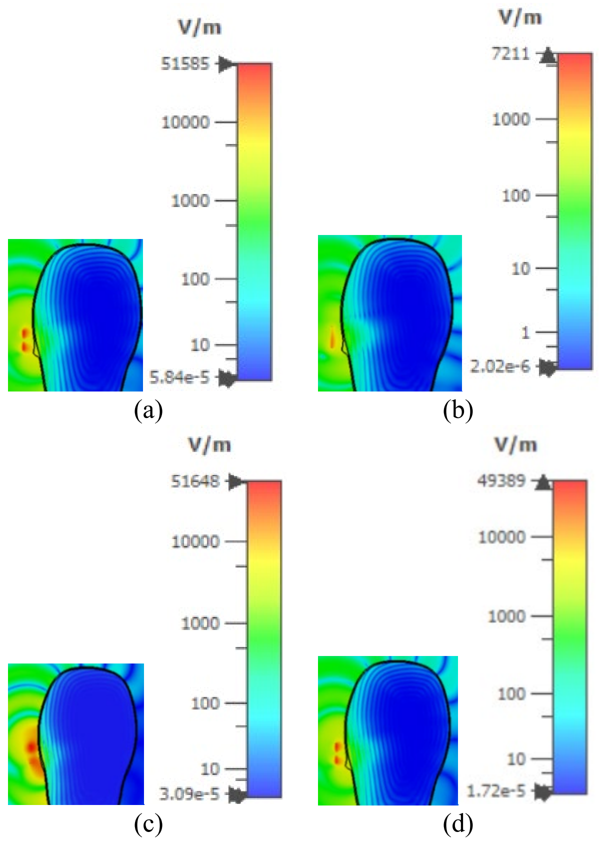

Figure 10. E-field intensity inside the head phantom for feeding located at: (a) P1, (b) P2, (c) P3, and (d) P4.

Figure 10 illustrates the electric field distribution within the head phantom at various feed positions. Figure 10 (c) shows the shallowest electric field penetration into the head phantom by the antenna with the P3 feed position, corresponding to the lowest SAR observed compared to the P1 and P4 feed points. In contrast, Figure 10 (b), representing the antenna with the P2 feed location, demonstrates a significantly weaker electric field surrounding the antenna, positioned near the head phantom, indicating poor radiation performance.

The final investigation involves varying the input power to determine the maximum permissible power of the conventional microstrip antenna, ensuring it remains safe and complies with SAR standard guidelines. The input power is varied from 0.06 W (17.78 dBm) to 0.08 W (19.03 dBm) to find the maximum permissible power for the proposed conventional microstrip antenna. The maximum permissible power for the proposed conventional microstrip antenna is 0.07 W (18.45 dBm), resulting in SARs of 1.56 W/kg for 1 g of tissue and 0.65 W/kg for 10 g of tissue, which do not exceed the SAR guidelines for either average tissue volume. The variation in input power results is tabulated in Table 3.

Table 4 presents a comparison between the proposed SAR assessment of the conventional microstrip antenna and the previous works. Most previous works presented a modified antenna structure [7], [13], and analyzed the SAR performance using the designs with line-type feeding [7], [13], [14], [16], [17], [18]. Thus, the SAR results presented in this study provide crucial baseline data for a conventional microstrip antenna utilizing a coaxial feeding method, particularly for future comparisons with modified antenna designs that have predominantly employed line-feeding methods in previous studies.

Table 3. Variation of the microstrip antenna input powers with SAR performance

Power (W)	SAR (W/kg)	
	1 g of tissue	10 g of tissue
0.06	1.34	0.55
0.07	1.56	0.65
0.08	1.79	0.74

Table 4. Comparison of the proposed work and its findings with previous works

Ref / Year	Freq (GHz)	Type of Microstrip Antenna	Type of feeding	Gain (dB) / Eff (%)	SAR 1g / 10 g (W/kg)
[7] / 2024	3.1-10.6	Hexagonal-shaped antenna	Line-feeding	8.05 / -	0.013/ 0.008
[13] / 2025	3.3	U-shaped semi-circular slot antenna	Line-feeding	7.47 / 67	0.095/ 0.036
[14] / 2023	28	Conventional	Line-feeding	7.3 / 89.4	1.68 / 0.121
[16] / 2023	3.5	Conventional	Line-feeding	7.43 / -	-
[17] / 2023	3.5	Conventional	Line-feeding	6.05 / -	-
[18] / 2023	3.5	Conventional	Line-feeding	2.2 / 56.25	-
Proposed Work	3.5	Conventional	Coaxial feeding	2 / 35	1.56 / 0.6

4. CONCLUSION

A microstrip antenna utilizing a coaxial feeding, which operates at 3.5 GHz with SAR analysis, has been presented. The antenna is designed based on the basic conventional microstrip patch structure with a coaxial feeding analysis, where the ideal feeding position is determined to ensure the antenna operates effectively at 3.5 GHz with good impedance matching. The results of S_{11} indicate that the microstrip antenna performs well, demonstrating good impedance matching when the coaxial feeding location is located at P3 (10 mm, -6 mm). It can also be noticed that the presence of the head phantom can affect the antenna performance, causing a slight shift in resonant frequency and alteration of the radiation pattern. These are due to the conductivity characteristic inside the human tissue, and the human tissue absorbs the power radiated by the antenna. The result shows that SAR is also affected by the location of the feeding. The antenna with the best position of the feeding, P3 (10 mm, -6 mm), demonstrated that 0.25 W (23.98 dBm) is too high to be used as an input power exceeding the exposure limit. The maximum permissible power that can be used is 0.07 W (18.45 dBm), which corresponds to the maximum safe range according to the SAR standard, with 1.56 W/kg and 0.65 W /kg for the respective 1 g and 10 g of tissue. Thus, this microstrip antenna functions safely and efficiently by employing the appropriate input power, making it suitable for any applications involving human proximity. Furthermore, the SAR results obtained in this study provide valuable baseline data for conventional coaxially fed microstrip antennas and can serve as a useful reference for future investigations on SAR performance.

ACKNOWLEDGMENT

The authors acknowledge the financial support from the Ministry of Higher Education through the HICoE Grant (4J613) and FRGS (FRGS/1/2022/TK07/UTM/02/58), and Universiti Teknologi Malaysia (UTM) via the UTM Nexus Scholarship.

REFERENCES

[1] A. Singh and S. Joshi, “Design of Y-shaped tri-band rectangular slot DGS patch antenna at sub-6 GHz frequency range for 5G communication,” *J. Eng. Appl. Sci.*, vol. 71, no. 1, pp. 1–17, 2024, doi: 10.1186/s44147-024-00476-w.

[2] D. Hagarty, S. Ajmeri, and A. Tanwar, *Synchronizing 5G Mobile Networks*. Cisco Press, 2021. [Online]. Available: https://www.vlebooks.com/vleweb/product/openreader?id=none&isbn=9780136836278

[3] M. S. Rana and M. M. R. Smieee, “Design and analysis of microstrip patch antenna for 5G wireless communication systems,” *Bull. Electr. Eng. Informatics*, vol. 11, no. 6, pp. 3329–3337, 2022, doi: 10.11591/eei.v11i6.3955.

[4] T. D. Kumar, M. S. S. S. Srinivas, P. S. R. Chowdary, M. Deepak, R. A. Varma, and T. S. Swaroop, “Design and Development of Compact Microstrip Patch Antenna with DGS for Wireless Applications,” *2024 IEEE Wirel. Antenna Microw. Symp. WAMS 2024*, pp. 1–4, 2024, doi: 10.1109/WAMS59642.2024.10528105.

[5] H. El-Hakim and H. A. Mohamed, “Synthesis of a Multiband Microstrip Patch Antenna for 5G Wireless

Communications," *J. Infrared, Millimeter, Terahertz Waves*, vol. 44, no. 9–10, pp. 752–768, 2023, doi: 10.1007/s10762-023-00937-y.

[6] M. S. Rana *et al.*, "A review on microstrip patch antenna for wireless communication systems at 3.5 GHz," *Bull. Electr. Eng. Informatics*, vol. 13, no. 4, pp. 2397–2407, 2024, doi: 10.11591/eei.v13i4.5941.

[7] K. V. Karad *et al.*, "A SAR analysis of hexagonal-shaped UWB antenna for healthcare applications," *Eurasip J. Wirel. Commun. Netw.*, vol. 2024, no. 1, 2024, doi: 10.1186/s13638-024-02405-0.

[8] International Commission on Non-Ionizing Radiation Protection, *ICNIRP Guidelines for limiting exposure to electromagnetic fields (100 kHz to 300 GHz)*, vol. 118, no. 5. 2020. doi: 10.1097/HP.0000000000001210.

[9] F. C. Commission, "Evaluating Compliance with FCC Guidelines for Human Exposure to Radiofrequency Electromagnetic Fields Supplement C," *Fed. Commun. Comm. Off. Eng. Technol.*, vol. 65, pp. 1–53, 2001.

[10] M. E. Karim and A. B. M. Aowlad Hossain, "SAR Analysis of Human Head Model Using Common Antennas of 4G LTE Mobile Communications," *2021 4th Int. Conf. Electr. Comput. Commun. Technol. ICECCT 2021*, pp. 1–5, 2021, doi: 10.1109/ICECCT52121.2021.9616924.

[11] S. S. Islam, A. Chowdhury, N. Paul, and S. Ahmed, "Electromagnetic Absorption Comparison of Dipole and Microstrip Patch Antenna in the Human Head," *2018 9th IEEE Annu. Ubiquitous Comput. Electron. Mob. Commun. Conf. UEMCON 2018*, pp. 1038–1041, 2018, doi: 10.1109/UEMCON.2018.8796804.

[12] H. Kaschel, C. Ahumada, and R. Osorio-Comparan, "Design and comparison of two types of antennas in the 2.45 GHz band to calculate the SAR," *2021 IEEE Int. Conf. Autom. Congr. Chil. Assoc. Autom. Control. ICA-ACCA 2021*, pp. 1–6, 2021, doi: 10.1109/ICAACCA51523.2021.9465175.

[13] R. W. Abd-Elsalam, H. E. Seleem, M. M. Abd-Elnaby, and A. H. Hussein, "Low SAR compact wideband/dual-band semicircular slot antenna structures for sub-6 GHz 5G wireless applications," *Eurasip J. Wirel. Commun. Netw.*, vol. 2025, no. 1, 2025, doi: 10.1186/s13638-024-02424-x.

[14] H. A. Al-Tayyar and Y. E. M. Ali, "Compact 28GHz Microstrip Patch Antenna Design with Reduced SAR for 5G Applications," *Math. Model. Eng. Probl.*, vol. 10, no. 5, pp. 1866–1872, 2023, doi: 10.18280/mmep.100540.

[15] A. Ahmed, N. I. Mohd Razali, N. Seman, N. A. Mohammad, and N. N. N. A. Malik, "5G Electromagnetic Field Exposure at 26 GHz: Absorbed Power Density Assessment," *IEEE Antennas Propag. Soc. AP-S Int. Symp.*, pp. 2769–2770, 2024, doi: 10.1109/AP-S/INC-USNC-URSI52054.2024.10686312.

[16] M. S. Rana, T. A. Fahim, B. Ghosh, and M. M. Rahman, "Microstrip patch antenna design and simulation for S-band wireless applications operating at 3.5 GHz," *Bull. Electr. Eng. Informatics*, vol. 12, no. 6, pp. 3428–3437, 2023, doi: 10.11591/eei.v12i6.5626.

[17] S. Rana, N. Khurshid, S. K. Joy, S. I. Sourav, J. Hassan, and J. Nazmul, "A 3.5 GHz microstrip patch antenna design and analysis for wireless applications," *Indones. J. Electr. Eng. Comput. Sci.*, vol. 32, no. 2, pp. 828–837, 2023, doi: 10.11591/ijeecs.v32.i2.pp828-837.

[18] C. Ramakrishna, A. Krishna Chaitnaya Varma, R. Orugu, V. V. S. Srinivas Ch, K. V. Subba Reddy M, and V. Rao Ch, "Design of Microstrip Patch Antenna at 3.5 GHz Frequency Using FEKO Simulation," *2023 2nd Int. Conf. Electr. Electron. Inf. Commun. Technol. ICEEICT 2023*, pp. 1–5, 2023, doi: 10.1109/ICEEICT56924.2023.10157700.

[19] A. A. Samat, D. N. A. Zaidel, D. A. A. Mat, M. R. M. Sharip, I. I. Muhamad, and Y. L. Then, "Surface Current Distribution and Performance Analysis of Different Feeding Techniques for Microstrip Patch Antenna," *2020 13th Int. UNIMAS Eng. Conf. EnCon 2020*, pp. 13–17, 2020, doi: 10.1109/EnCon51501.2020.9299340.

[20] A. F. Pazil, N. Huda, A. Rahman, N. Ramli, N. Farhana, and H. A. Razak, "Comparative Analysis on Different Feeding Techniques of Textile Antenna for Gps-L1 Application," *J. Eng. Technol. Adv.*, vol. 6, no. 1, 2021, doi: 10.35934/segi.v6i1.20.

[21] N. A. Mohd Shukor and N. Seman, "5G planar branch line coupler design based on the analysis of dielectric constant, loss tangent and quality factor at high frequency," *Sci. Rep.*, vol. 10, no. 1, pp. 1–15, 2020, doi: 10.1038/s41598-020-72444-2.

[22] C. A. Balanis, *Antenna Theory: Analysis and Design*, Third Edit. John Wiley & Sons, Inc., Hoboken, New Jersey, 2005.

[23] N. I. Mohd Razali, N. Seman, and N. A. Muhammad, "Design and SAR of Sub-6 GHz Multiband Antenna with Slots and Defected Ground Plane," pp. 9–10, doi: 10.1109/TAP.2007.893427.

[24] C. A. Balanis, *Modern Antenna Handbook*. John Wiley & Sons, 2011. [Online]. Available: https://books.google.com.my/books?id=UYpV8L8GNCwC&pg=RA2-PA31&dq=radiation+efficiency+depend+on+reflection+coefficient&hl=en&newbks=1&newbks_redir=0&sa=X&ved=2ahUKEwiHv6r5pZGFAxWwn2MGHT-8B70Q6AF6BAgKEAI#v=onepage&q=radiation efficiency depend on reflectio

[25] N. Inshirah, M. Razali, N. Seman, and N. A. Muhammad, "Simple dual-slot L-shaped microstrip antenna for sub-6 GHz," *Sci. Rep.*, vol. 16, pp. 1–15, 2026.

[26] M. V. Mokal, P. S. R. Gagare, and R. P. Labade, "Analysis of Micro strip patch Antenna Using Coaxial feed and Micro strip line feed for Wireless Application," *IOSR J. Electron. Commun. Eng.*, vol. 12, no. 3, pp. 36–41, 2017, doi: 10.9790/2834-1203033641.

[27] N. I. Mohd Razali, N. Seman, and N. A. Muhammad, "Scientific Reports Article in Press Simple dual-slot L-shaped microstrip antenna for sub-6 GHz," *Sci. Reports*, 2026.

[28] N. I. Mohd Razali, N. Seman, and N. A. Muhammad, "Specific Absorption Rate and Maximum Permissible Input Power of Planar Inverted-F Antennas," *Results Eng.*, vol. 26, no. March, pp. 1–9,

2025, doi: 10.1016/j.rineng.2025.104897.

[29] N. I. Mohd Razali, N. Seman, and T. H. Chua, "Designs of rectangular-shaped planar inverted-F antennas at mobile operating frequencies with different ground plane techniques," *Indones. J. Electr. Eng. Comput. Sci.*, vol. 15, no. 2, pp. 927–935, 2019, doi: 10.11591/ijeecs.v15.i2.pp927-935.

[30] H. R. Zu, B. Wu, Y. H. Zhang, Y. T. Zhao, R. G. Song, and D. P. He, "Circularly Polarized Wearable Antenna with Low Profile and Low Specific Absorption Rate Using Highly Conductive Graphene Film," *IEEE Antennas Wirel. Propag. Lett.*, vol. 19, no. 12, pp. 2354–2358, 2020, doi: 10.1109/LAWP.2020.3033013.

[31] W. L. Stutzman and G. A. Thiele, *Antenna Theory and Design*, Third Edit. Wiley, Hoboken, NJ, 2013. [Online]. Available: https://www.google.com.my/books/edition/Antenna_Theory_and_Design/xhZRA1K57wIC?hl=en&gbpv=1&dq=antenna+power+radiation+is+reduced+due+to+absorb+by+human+body&pg=PA524&printsec=frontcover

[32] T. Aishwarya and P. Das, "A FSS integrated wearable modified bow-tie antenna for biomedical applications," *Results Eng.*, vol. 26, no. March, 2025, doi: 10.1016/j.rineng.2025.104894.

[33] P. Pradeep, J. S. Kottareddygari, and C. S. Paidimarry, "Design of a Dual-Band Monopole Antenna for Internet of Things and Sub-6 GHz 5G Applications," *2024 IEEE Wirel. Antenna Microw. Symp. WAMS 2024*, pp. 1–4, 2024, doi: 10.1109/WAMS59642.2024.10528093.

[34] *IEEE Standards for Safety Levels with Respect to Human Exposure to Electric, Magnetic, and Electromagnetic Fields, 0 Hz to 300 GHz, IEEE Std C95.1TM-2019 (Revision of IEEE Std C95.1-2005/ Incorporates IEEE Std C95.1-2019/Cor 1-2019) This*. 2019.